Surface Science 641 (2015) 282–288

Contents lists available at ScienceDirect

Surface Science

journal homepage: www.elsevier.com/locate/susc

Separation of the attractive and repulsive contributions to the adsorbate–adsorbate interactions of polar adsorbates on Si(100)

Ying-Hsiu Lin, Horng-Tay Jeng, Deng-Sung Lin *

Department of Physics, National Tsing Hua University, 101 Section 2, Kuang-Fu Road, Hsinchu 30013, Taiwan

ARTICLE INFO

Available online 9 December 2014

Keywords:
Adsorbate–adsorbate interactions
Density functional theory calculations
Polar molecules
Si(100) surface

ABSTRACT

Dissociative adsorption of H_2O, NH_3, CH_3OH and CH_3NH_2 polar molecules on the Si(100) surface results in a 1:1 mixture of two adsorbates (H and multi-atomic fragment A = OH, NH_2, CH_3O, CH_3NH, respectively) on the surface. By using density functional theory (DFT) calculations, the adsorption geometry, the total energies and the charge densities for various possible ordered structures of the mixed adsorbate layer have been found. Analyzing the systematic trends in the total energies unveils concurrently the nearest-neighbor interactions E_{NN} and the next nearest-neighbor interactions E_{NNN} between two polar adsorbates A. In going from small to large polar adsorbates, E_{NN}'s exhibit an attractive-to-repulsive crossover behavior, indicating that they include competing attractive and repulsive contributions. Exploration of the charge density distributions allows the estimation of the degree of charge overlapping between immediately neighboring A's, the resulting contribution of the steric repulsions, and that of the attractive interactions to the corresponding E_{NN}'s. The attractive contributions to nearest neighboring adsorbate–adsorbate interactions between the polar adsorbates under study are shown to result from hydrogen bonds or dipole–dipole interactions.

1. Introduction

It is well established that an adsorbate can interact attractively or repulsively with neighboring adsorbates. Taking the adsorption of organic molecules for example, several different origins of adsorbate–adsorbate interactions (AAIs) have been identified [1,2]. They include direct adsorbate–adsorbate steric repulsion, dipole–dipole interaction and hydrogen bonding. Some AAIs, such as that in the Al/Al(111) and Cu/Cu(111) systems, are mediated by the substrate through electronic effects on neighboring sites [3]. These AAIs may coexist and compete in strength with each other, depending on the specific adsorbates and surfaces involved. It has also been suggested that adsorbate-induced changes in surface polarization may play an important role in determining the two-dimensional ordering of organics on semiconductors [1,4]. Since we can only measure the total interaction between two adsorbates, the strength of these different interactions cannot be easily obtained quantitatively.

Recently, intermolecular hydrogen bonds have been shown to play a dominant role in determining the packing patterns in organic molecular monolayers [5]. Hydrogen bonds (H-bonds) are formed between a species with a polar $X^{\delta-}-H^{\delta+}$ bond and a species with a lone pair ($Y^{\delta-}$), i.e., $X^{\delta-}-H^{\delta+}\ldots Y^{\delta-}$, or simply X–H…Y. The most common species for X are fluorine, oxygen and nitrogen. However, X-ray and neutron diffraction studies have shown that crystals of various organic compounds exhibit close C–H…Y contacts which show all the stereochemical hallmarks of hydrogen bonds. A hydrogen bond is a special case of dipole forces and generally stronger than dipole–dipole interactions and dispersion forces. Typical energies for hydrogen bonds vary from very weak (20 meV) to extremely strong (>1.0 eV) and bond lengths (measured from the hydrogen atom) range typically between 1.6 and 2.6 Å, depends on bond strength, temperature, bond angle, and pressure [6,7]. H bonding involving the C–H group is usually weak with bond strength of 40 meV or less, because the C–H group is not so electronegative.

Many organic molecules are polar, with an OH or NH_2 ligand. Polar adsorbates can interact directly with each other to cause certain adsorbate orderings. Using DFT slab calculations, Cho et al. have shown that dissociated OH fragments from H_2O are attracted to each other by hydrogen-bonding [8]. The attractive interaction expectedly leads to the OH chain formation along the same side of a dimer row [9]. However, the zigzag patterns in which OH sites occupy alternatively opposite sides of the dimer rows were also found [10]. Methanol adsorption on the Si(100)-(2 × 1) surface was found to result in CH_3O and H on dangling bonds. The effects of the hydrogen position on the CH_3O adsorption energy were less than 0.20 eV [11]. Queeney et al. have combined infrared absorption spectroscopy measurements and density functional cluster calculations and shown that dissociative NH_3 adsorption yields the zigzag structure in which dissociated NH_2 species bind alternatively to the opposite side of Si dimers along a row [12]. A recent STM study by Hossain et al. has also demonstrated that dissociative NH_3 adsorption prefers the zigzag structure [13].

* Corresponding author.
E-mail address: dslin@phys.nthu.edu.tw (D.-S. Lin).

http://dx.doi.org/10.1016/j.susc.2014.12.002
0039-6028/

Nevertheless, Widjaja and Musgrave have predicted, by using DFT cluster calculations, the possibility of aligned structure formation by virtue of hydrogen bonding between dissociated NH_2 moieties [4]. Similarly, Cho and Kleinman have predicted that the alignment of dissociated CH_3NH moieties from CH_3NH_2 is due to the adsorbate-induced buckling switch. Conversely, a recent DFT-slab calculation result has suggested that both molecular and dissociative CH_3NH_2 adsorption structures at the saturation coverage prefer the zigzag arrangement due to adsorbate–adsorbate repulsion [14].

The diverged results mentioned above call for the need of further investigation on the AAIs. Previously a calculation scheme has been introduced to untangle concurrently various nearest-neighboring (NN) and next-nearest-neighboring (NNN) interactions due to steric repulsive interactions from atomic adsorbates [15]. As this investigation will demonstrate, a further development of this method allows a successful decomposition of AAIs into the attractive contribution and the steric repulsion for various multi-atomic adsorbates. Even though the decomposition method presented herein gives only a rough estimation, it provides new quantitative insight into the coexisting and competing nature of the AAIs between multi-atomic polar adsorbates.

2. Methods

DFT calculations were performed using Vienna Ab-initio Simulation Package (VASP) employing generalized gradient approximation of Perdew, Bruke, and Ernzerhof (PBE) functional [16–19]. The Si substrate was modeled by an 8-layer Si(100) slab with a lateral size of (4×2) unit cells. The bottom two layers in the $4 \times 2 \times 8$ slab with fixed at bulk positions and the surface terminated by hydrogen. A vacuum region of thickness 15 Å on top of the Si surface was included to form a supercell. Plane waves of kinetic energies up to 33 Ry were included [20]. The irreducible Brillouin zone was sampled with a $(16 \times 16 \times 1)$ Monkhorst–Pack mesh for 1×1 cells [21]. Geometry optimization was performed until the total energy converged to within 10^{-5} eV. Cell sizes were fixed to yield a Si lattice constant of 5.46 Å.

3. Results and discussion

A Si(100) $-$ (2×1) surface is composed of parallel rows of Si dimers [22,23]. A symmetric silicon dimer ($-$Si–Si$-$) has one dangling bond on each of the two dimer atoms; the two dangling bonds are referred to as a *dangling-bond pair* (DBP). The dangling bond orbits are half-filled and chemically active, offering a natural base for molecule adsorption. To further reduce the total energy, the two dimer atoms become buckled and the two dangling bonds in a DBP form a weak π-bond [24–26]. As theoretic studies have also shown, the surface energy can be lowered slightly further by relaxations, i.e., the buckling directions in neighboring dimers are alternative [27,28]. The $p(2 \times 2)$ and $c(4 \times 2)$ structures consisting of alternating dimers are seen in the STM images and the intrinsic properties of the clean Si(100) become quite complex [29,30]. As reported elsewhere [31], our calculations showed that the buckled phase is favored by 0.08 eV per (1×1) supercell over the symmetric (2×1) phase and that other structure parameters are consistent with previous findings [26,28,32].

3.1. Interaction model and energy calculations

The reactions of molecules M with Si(100) (M = water (H_2O) [33], ammonia (NH_3), methanol (CH_3OH) [34], and methylamine (CH_3NH_2) [35] involve dissociation of the molecule into fragments H and A, where A are, respectively, OH (hydroxyl), NH_2 (amidogen), CH_3O (methoxy), and CH_3NH (methylamino) radicals. Since both fragments H and A are highly reactive radicals, they each chemisorb on a half-filled dangling bond. Upon sufficient exposure of the gas molecules, the surface became fully saturated with mixed (H–Si and A–Si) surface species while the dimer bonds remained unbroken as observed experimentally; the H- and A-terminated surface is denoted as Si(100):AH. If the mixed adsorbates form ordered structures, the basic building blocks for the Si(100):AH surface are either mixed occupation dimers (MOD) A–Si–Si–H (AH for short) or H–Si–Si–A (HA), or paired occupation dimers (POD) A–Si–Si–A (AA) or H–Si–Si–H (HH). Following a previous report [15], eight different ordered adsorbate structures can be formed as listed in Table 1 in a (4×2) cell. Labels "m" and "p" in Table 1 indicate that the structure is formed, respectively, by MODs and PODs. The (2×1)-p structure describes a surface where the top half is Si(100)-(2×1): A and the bottom half is Si(100)-(2×1):H.

One of the eight ordered structures, i.e. (4×1)-m, for the relaxed Si(100):AH surface is displayed in Fig. 1. In this structure, A's occupy the same side of a dimer row, forming an A-row along [0, 1, -1]. Evidently, each adsorbate A in Fig. 1, is oriented in such a way that one of its hydrogen atoms is close to the lone pair of electrons of an oxygen or nitrogen atom in the nearest neighboring fragment in the same A-row or in the neighboring A-row. As Fig. 1(a) exhibits, A_1 and A_2 in the same OH-row line up to form short H…O bonds; the hydrogen bond length between H and O in the same OH-row is denoted by d_α. On the other hand, Fig. 1(b) showed that, for adsorbates NH_2, A_1 and A_3 with the shortest H…N bond reside in neighboring rows, which denoted as $d_{\beta m}$.

Table 1
Atomic arrangements and interaction energies for mixed adsorbates A and H in a 4×2 unit cell on Si(100). Labels "m" and "p" in Row 1 and 4 indicate that the structure is formed, respectively, by MODs and PODs. The energy for (2×1)-p, $E_{8,AH}$, is the mean of the two energies for A- and H-terminated (2×1) structure, respectively. Also listed are calculated bond directions (in degree, see text).

Structure i	1: (2×2)-m	2:c(4×2)-m	3:(2×1)-m	4:(4×1)-m	5:c(4×2)-p	6:(2×2)-p	7:(4×1)-p	8:(2×1)-p
Atomic arrangement in a (4×2) cell	HA_1 HA_3 A_2H A_4H	A_1H HA_3 HA_2 A_4H	HA_1 HA_3 HA_2 HA_4	HA_1 A_3H HA_2 A_4H	HH A_3A_4 A_1A_2 HH	HH HH A_1A_2 A_3A_4	HH A_1A_3 HH A_2A_4	A_1A_3 A_5A_7 A_2A_4 A_6A_8 + HH HH HH HH
$E_{i,AH}$ interaction energy per 4×2	$4\eta_{AH} + 8\alpha_{AH} + 4\beta_{AH} + 4\rho_{AA} + 4\rho_{HH} + 4\gamma_{AA} + 4\gamma_{HH}$	$4\eta_{AH} + 8\alpha_{AH} + 2\beta_{AA} + 2\beta_{HH} + 4\rho_{AA} + 4\rho_{HH} + 8\gamma_{AH}$	$4\eta_{AH} + 4\alpha_{AA} + 4\alpha_{HH} + 4\beta_{AH} + 8\rho_{AH} + 8\gamma_{AH}$	$4\eta_{AH} + 4\alpha_{AA} + 4\alpha_{HH} + 2\beta_{AA} + 2\beta_{HH} + 8\rho_{AH} + 4\gamma_{AA} + 4\gamma_{HH}$	$2\eta_{AA} + 2\eta_{HH} + 8\alpha_{AH} + 4\beta_{AH} + 8\rho_{AH} + 4\gamma_{AA} + 4\gamma_{HH}$	$2\eta_{AA} + 2\eta_{HH} + 8\alpha_{AH} + 2\beta_{AA} + 2\beta_{HH} + 8\rho_{AH} + 8\gamma_{AH}$	$2\eta_{AA} + 2\eta_{HH} + 4\alpha_{AA} + 4\alpha_{HH} + 4\beta_{AH} + 4\rho_{AA} + 4\rho_{HH} + 8\gamma_{AH}$	$2\eta_{AA} + 2\eta_{HH} + 4\alpha_{AA} + 4\alpha_{HH} + 2\beta_{AA} + 2\beta_{HH} + 4\rho_{AA} + 4\rho_{HH} + 4\gamma_{AA} + 4\gamma_{HH}$
$E_i = E_{i,AH} - E_{8,AH}$	$-2\eta_{AA} - 4\alpha_{AA} - 2\beta_{AA\text{-}m}$	$-2\eta_{AA} - 4\alpha_{AA} - 4\gamma_{AA\text{-}m}$	$-2\eta_{AA} - 2\beta_{AA\text{-}m} - 4\rho_{AA} - 4\gamma_{AA\text{-}m}$	$-2\eta_{AA} - 4\rho_{AA}$	$-4\alpha_{AA} - 2\beta_{AA\text{-}p} - 4\rho_{AA}$	$-4\alpha_{AA} - 4\rho_{AA} - 4\gamma_{AA\text{-}p}$	$-2\beta_{AA\text{-}p} - 4\gamma_{AA\text{-}p}$	0
θ_{OH}	$A_{1,2,3,4}$: -90	$A_{1,2,3,4}$: 180	$A_{1,2,3,4}$: -90	$A_{1,2}$: -90 $A_{3,4}$: 90	$A_{1,2,3,4}$: 180	$A_{1,2,3,4}$: 180	$A_{1,2}$: 90 $A_{3,4}$: -90	$A_{1,2,5,6}$: 90 $A_{3,4,7,8}$: -90
$(\theta_{NH1}, \theta_{NH2})$	$A_{1,2,3,4}$: (40, -110)	$A_{1,4}$: (40, -110) $A_{2,3}$: (25, -100)	$A_{1,2,3,4}$: (15, -120)	$A_{1,2}$: (20, -120) $A_{3,4}$: (40, -110)	$A_{1,3}$: (40, -110) $A_{2,4}$: (25, -105)	$A_{1,3}$: (40, -110) $A_{2,4}$: (25, -105)	$A_{1,2}$: (30, -120) $A_{3,4}$: (20, -105)	$A_{1,2,5,6}$: (30, -120) $A_{3,4,7,8}$: (25, -100)

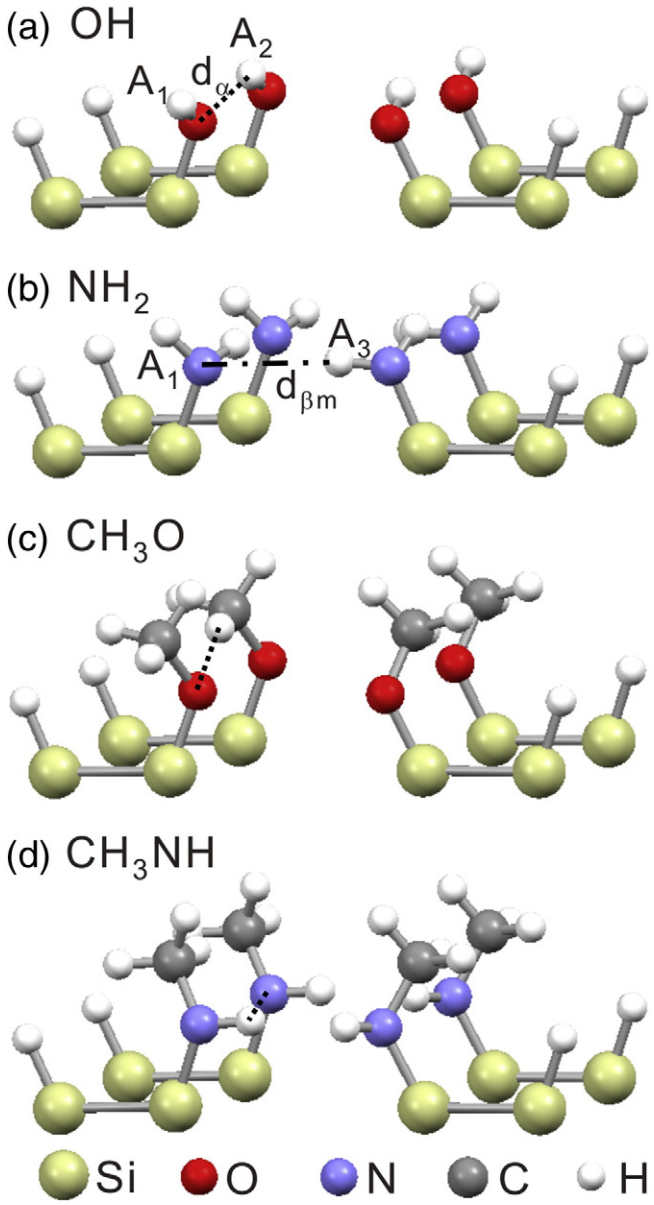

Fig. 1. Relaxed (4 × 1)-m structure for various adsorbates as indicated. A dot-line (d_α) and a dashed dot one ($d_{\beta m}$) indicate the distances between an electronegative O (or N) atom and proton in two nearest neighboring adsorbates in the same A-row or in the neighboring A-row.

Other structures also exhibit similar tendencies in adsorbate orientations; the orientation of an adsorbate A is defined by its O–H (or N–H) bond directions, as shown in Fig. 2 and listed in Table 1. The trend in adsorbate orientations can be attributed to the formation of hydrogen bonds (O–H…O and N–H…N) between two organic moieties as will be further discussed in Section 3.4. Notably not all the orientations for the four organic moieties in eight arrangements are the same (see θ_{OH}, θ_{NH1}, and θ_{NH2} in Table 1) and, therefore, the notations of interaction energy for ith structure should be changed accordingly. However, to keep the notation and discussion simple, the notations of interaction energy herein disregard the detailed geometry of adsorbates A.

The calculated adsorption energies for the ith structure of eight structures, $E_{ads,\,i}$, are listed in Table 2. The adsorption energy is defined as

$$E_{ads,i} = -E_{Si(100):AH,i} + E_{Si(100)} + E_M$$

where $E_{Si(100):AH,\,i}$ and $E_{Si(100)}$ are the respective calculated total energies of Si(100) with and without adsorbed species A. E_M is the total energy of four isolated M's before adsorption. The symbol M is dropped in $E_{ads,\,i}$, again to keep the notation short and general. Noticeably, $E_{ads,\,i}$ is slightly different for each structure. The chemical energy components (including the dissociation energies of the adsorbed molecules and the fragment-surface bond energies) presumably are the same for all structure and can be eliminated by using a relative energy scale, i.e. $E_i = E_{ads,\,i} - E_{ads,\,8}$. The mean of the two energies for A- and H-terminated (2 × 1) structure, $E_{ads,\,8}$ is used as a reference to minimum the interaction terms listed in Table 1. The relative energies E_i's involving AAIs have been calculated from data in Table 2 and plotted in Fig. 3. E_i's for the polar fragments OH and NH_2 are positive and show several analogous trends:

1. The relative energies are in the same order from the highest to lowest: $E_1 > E_2 > E_3 \approx E_4$ for the MOD configurations and $E_5 > E_6 > E_7 \approx E_8$ for the POD configurations. The energy gap between E_2 and E_3 for OH/NH_2 implied that adsorbates OH/NH_2 appear to align along [0, 1, −1], while the energy gap between E_5 and E_6 appear to align along [0, 1, 1]. In other words, an OH or NH_2 adsorbate appears to have an attractive interaction with another. Calculated results (Table 3) will confirm this observation.
2. The relative lower energies $E_3 \approx E_4 \approx E_7 \approx E_8$ for OH and $E_3 \approx E_4 \approx E_6 \approx E_7 \approx E_8$ for NH_2 suggest that the adsorbate fragments OH or NH_2, are energetically more desirable to cluster together than separate; with similar energies, we expected that no specific atomic arrangements with large area can be observed. However, the alignment of dissociated NH_2 moieties on the same side to form chain-like structure and on the opposite side to yield zigzag structure along a Si dimer row were both observed by STM. This occurrence indicates that the thermodynamic consideration alone is not sufficient to determine the adsorbate structure and that the kinetic barrier comes into play [11].

Fig. 3 also showed that the relative energy for CH_3O and CH_3NH:

1. The relative energies of CH_3O from the lowest to highest: $E_3 \approx E_4 < E_1 \approx E_2$ for the MOD configurations, suggest that adsorbate CH_3O appears to align along [0, 1, −1], which have an overall attractive interaction with another. Calculated results (Table 3 in Section. 3.2) will confirm this observation. Since the relative energies of $E_5 \approx E_6 \approx E_7 \approx E_8$ for CH_3O are higher than E_1, E_2, E_3, and E_4, the formation of the two MODs HA upon chemisorption of two CH_3OH molecules is energetically preferable to that of two different PODs AA and HH. Calculated results for the inter-dimer interaction $\eta_{|AA}$ (Table 3) will confirm this observation.
2. The relative energies of CH_3NH from the lowest to highest: $E_1 < E_2 < E_3 \approx E_4$ for the MOD configurations and $E_5 < E_6 < E_7 < E_8$ for the POD configurations. E_8 has the highest value among the eight E_i's. Accordingly, the segregation into the hydrogen- and methylamino-terminated domains is not energetically favorable, even when it is kinetically plausible. On the other hand, the (2 × 2)-m structure has the lowest interaction energies. This indicates the zigzag arrangement of adsorbate CH_3NH is more favorable, suggesting that an adsorbate CH_3NH has a repulsive interaction with another.

3.2. Calculated adsorbate–adsorbate energy in various directions

As described in Section. 3.1, all the eight structures have the same chemical bonding between each adsorbed fragment A and a Si dimer atom. Yet, the adsorption energies $E_{ads,\,i}$ are different in the eight structures and have the similar trends for different polar fragments. These findings suggest that the differences in $E_{ads,\,i}$ for different structures are due to AAI between adsorbates. Previous studies have demonstrate that DFT calculations can resolved the pair-wise

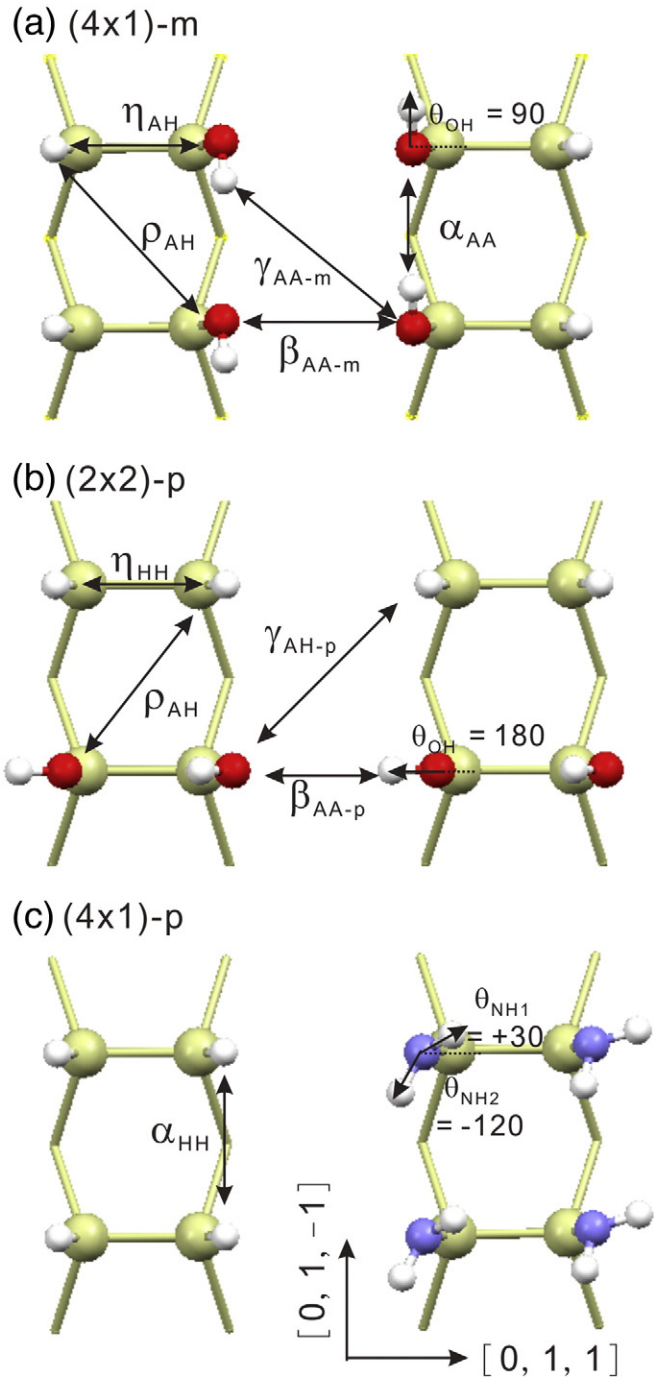

Fig. 2. Top view of a (4×2) unit cell used to calculate AAIs. η_{AH}, η_{HH}, η_{AA} (or η) = nearest-neighbor interaction (E_{NN}) in a dimer; α_{AH}, α_{HH}, α_{AA} (or α) = E_{NN} in two neighboring dimers in the same row; β_{AH}, $\beta_{AA\text{-}p}$ (or β_p), $\beta_{AA\text{-}m}$ (or β_m) = E_{NN} in two neighboring rows. Those between two next-nearest neighbors are labeled as ρ and γ. The orientations (solid arrows) θ_{OH} for O–H (a–b) and (θ_{NH1}, θ_{NH2}) for N–H (c) are relative to dimer bond direction [0, 1, 1].

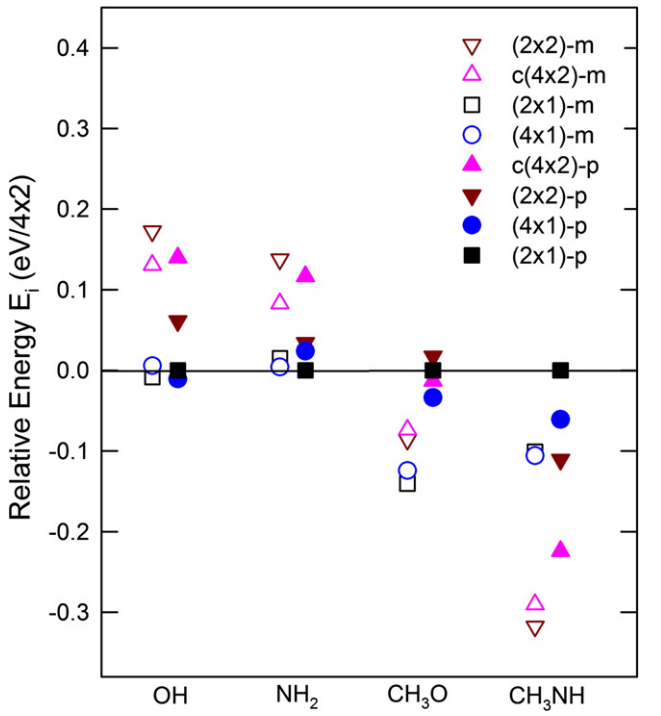

Fig. 3. Relative energy E_i for mixed hydrogen and polar fragments on Si(100) for various adsorbate structures as labeled. Energies refer to that of the (2×1)-p structure, which is set to zero.

interactions and higher ordered terms between individual adatoms [36,37]. Herein, a similar concept is employed using approximative truncated expansion of the interaction energies in terms of pair interactions within the third neighboring distance. Several fundamental AAIs between the two adsorbate radicals for the above-mentioned structures are depicted in Fig. 2: for example, η_{AH} is the nearest-neighbor interaction (E_{NN}) between adsorbates A and H in a dimer; α_{AA} (or α for simplicity), E_{NN} between two adsorbates A in two neighboring dimers in the same row; $\beta_{AA\text{-}m}$ (or β_m), E_{NN} between two adsorbates A in two MODs in neighboring rows; ρ_{AH}, next nearest-neighbor interaction (E_{NNN}) between adsorbates A and H in two neighboring dimers in the same row; and $\gamma_{AA\text{-}p}$ (or γ_p), E_{NNN} between two adsorbates A in two PODs in neighboring rows. By neglecting the difference between β_m and β_p and the difference between γ_m and γ_p, each of the total adsorbate–adsorbate interaction energy $E_{i,AH}$ for the eight structures is also listed in Row 3, Table 1. Particularly, the energy for (2×1)-p, $E_{8,AH}$, is the mean of the two energies for A- and H-terminated (2×1) structure, respectively. Because the interactions between H and A are presumably negligible [15], we can further reduce the number of terms in the interactions by assuming $\pi_{HH} = \pi_{AH} = 0$, where $\pi = \eta$, α, β, ρ, or γ. With these simplifications, the relative interaction energies E_i for the mixed hydrogen-organic moiety terminated surfaces Si(100):AH contain only the interactions between two adsorbates A as listed in Table 1. From Table 1, π_{AA} can be found:

$$\alpha = \alpha_{AA} = (-E_1 - E_2 + E_3 + E_4 - E_5 - E_6 + E_7 + E_8)/16 \quad (1)$$

Table 2
Calculated adsorption energies $E_{ads,\,i}$ (meV per (4×2) cell) of the ith adsorbate structure for various polar molecules.

Structure i	1 (2×2)-m	2 c(4×2)-m	3 (2×1)-m	4 (4×1)-m	5 c(4×2)-p	6 (2×2)-p	7 (4×1)-p	8 (2×1)-p
H_2O	−10590.5	−10632.2	−10771.5	−10757.4	−10623.2	−10701.8	−10773.7	−10763.0
NH_3	−8895.6	−8950.6	−9018.16	−9029.2	−8916.72	−8999.22	−9009.62	−9033.42
CH_3OH	−10517.3	−10505.1	−10571.9	−10555.8	−10444.4	−10414.2	−10465.2	−10431.4
CH_3NH_2	−9033.4	−9006.2	−8816.8	−8821.7	−8940.2	−8826.5	−8776.8	−8715.9

Table 3
Calculated interaction energies, E_{NN}'s and E_{NNN}'s, respectively between two nearest neighbors and two next nearest neighbors of the same kind (A). The interaction energies are in units of meV. See the text for details.

Adsorbate A	E_{NN} (meV)				E_{NNN} (meV)		
	η	α	β_p	β_m	ρ	γ_p	γ_m
OH	−12.9	−32.4	−17.0	−6.9	5.9	11.2	7.0
NH_2	−5.0	−20.5	−26.6	−16.5	4.6	7.3	5.5
CH_3O	45.0	−9.0	16.0	7.1	4.2	0.4	0.5
CH_3NH	35.9	42.2	43.7	5.6	−7.9	−6.6	−4.0

Table 4
Calculated critical isovalues n_c of electron density between two adsorbates of the same kind (A) and corresponding adsorbate repulsion energies interpolated from that of halogens as indicated in Fig. 5. The electron clouds of CH_3NH along the [0,1,1] direction overlap at two areas as seen in Fig. 4(d) and therefore, two isovalues $n_{c,\beta}$ are listed. The corresponding electron overlapping is the mean of two isovalues. See the text for details.

A	n_c (e/Å^3)		Adsorbate repulsion E_{rep} (meV)		
	$n_{c,\alpha}$	$n_{c,\beta}$	$E_{rep,\ \alpha}$	$E_{rep,\ \beta m}$	$E_{rep,\ \beta p}$
OH	0.0164	0.0087	19.6	15.4	20.0
NH_2	0.0236	0.0154	27.8	19.2	23.2
CH_3O	0.0501	0.0170	69.4	20.2	24.1
CH_3NH	0.0578	$\frac{(0.0180+0.0275)}{2}$	85.7	24.2	27.9

$$\rho = \rho_{AA} = (E_1 + E_2 - E_3 - E_4 - E_5 - E_6 + E_7 + E_8)/16 \quad (2)$$

$$\beta_m = \beta_{AA\text{-}m} = (-E_1 + E_2 - E_3 + E_4)/4 \quad (3)$$

$$\gamma_m = \gamma_{AA\text{-}m} = (E_1 - E_2 - E_3 + E_4)/8 \quad (4)$$

$$\beta_p = \beta_{AA\text{-}p} = (-E_5 + E_6 - E_7 + E_8)/4 \quad (5)$$

$$\gamma_p = \gamma_{AA\text{-}p} = (E_5 - E_6 - E_7 + E_8)/8. \quad (6)$$

The bond angle and charge distribution for an adsorbate A in an MOD are expected to be slightly different to that in a POD. In Eqs. (3), (4), (5) and (6), additional labels m and p are added on to the interaction energies β's and γ's because they can be similarly derived independently for the MOD and POD.

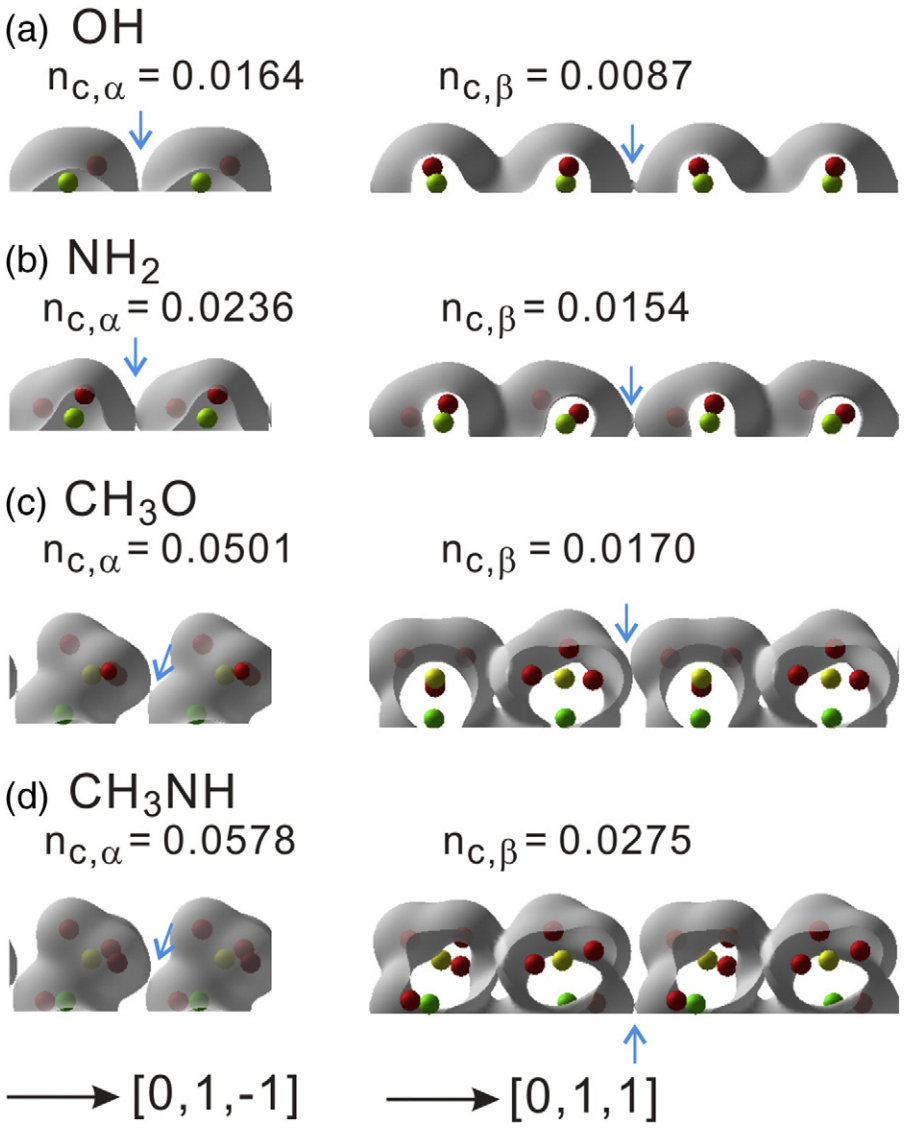

Fig. 4. Side view of isosurfaces of charge density for various polar moieties A on Si(100). With an isovalue $n_{c,\alpha}$ and $n_{c,\beta}$ (e/Å^3) as indicated, the two isosurfaces of two neighboring adsorbates as labeled start to overlap along the dimer row direction [0, 1, −1] and the dimer bond direction [0, 1, 1], respectively. Blue arrows are guides to the contact points.

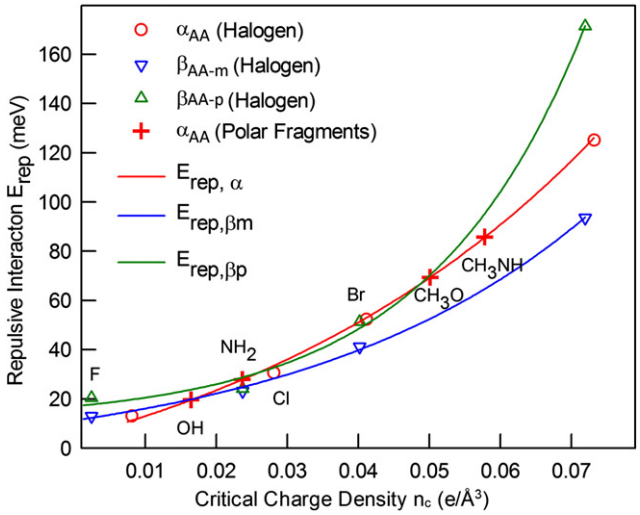

Fig. 5. Nearest-neighbor adsorbate repulsive interaction energies E_{rep} as a function of critical isovalue n_c between two halogens (open circle, triangle-up and triangle-down) and interpolated α_{AA} between two polar fragments (cross) of the same kind as labeled.

The interaction energies π_{AA} in Eqs (1–66) are listed in Table 3. Using the obtained π_{AA} ($\pi = \alpha, \beta, \rho,$ or γ), η_{AA} can equivalently be found by the following relations:

$$\eta = \eta_{AA} = \left(E_8 - 4\alpha - 2\beta_p - 4\rho - 4\gamma_p\right)/2 = \left(E_5 - 4\gamma_p\right)/2 = \left(E_6 - 2\beta_p\right)/2 = (E_7 - 4\alpha - 4\rho)/2. \quad (7)$$

Several combined indirect interactions such as substrate strains or electronic modulations are responsible for E_{NNN}. However, E_{NNN} are relatively small as Table 3 shows. E_{NN} for CH_3O and CH_3NH are almost all positive, similar to those found for halogen-terminated surface [13]. In other words, the AAIs are repulsive. This result may be similarly explained by the overlapping of the electrons from two neighboring adsorbates. However, E_{NN} for OH and NH_2 are negative, suggesting that the adsorbed fragments of OH or NH_2 effectively attract each other, in contrast to the halogens and larger polar fragments CH_3O and CH_3NH.

3.3. Estimation of the repulsive adsorbate–adsorbate interactions

Upon bonding to the surface, the above mentioned adsorbed fragments show no apparent chemical bonds between neighboring adsorbates, as judged by their separations. The nearest-neighbor repulsive interaction, E_{rep}, due to the Pauling repulsion of the overlapping of electrons from two neighboring adsorbates is universally present for all adsorbates. The larger the effective radius of the adsorbates, or more precisely, the resulting electron overlapping, the stronger the repulsive forces are. Since halogen adatoms adsorbed on the Si(100) surface can be sensibly viewed as spheres, the extent of electron overlapping has been shown to be in proportion to $\exp(R_A + R_B - d_{AB})$, where R_A and R_B are the ionic radii of the two interaction halogen atoms A and B, respectively, and d_{AB} is the calculated inter-nuclear distance between A and B [13]. The advantage of this method is that the estimation is achievable by using the ionic radii and calculated relaxed distance d_{AB} without more calculations. However, this straightforward approximation is not applicable to the non-spherical adsorbates, such as the multi-atomic adsorbates discussed herein.

One way to evaluate the extent of electron overlapping is to examine the critical isovalue of electron density n_c (e/Å^3) where the two isosurfaces of two neighboring adsorbates are in contact with each other. As Fig. 4 shows, along the [0,1,1] and [0,1, −1] directions, the electron isosurfaces of the two neighboring adsorbates contact with each other. Following the notations in Fig. 2, the contact point along the [0,1, −1] ([0,1,1]) direction is related to the α (β) interaction and the isovalue found is referred to as $n_{c,\alpha}$ ($n_{c,\beta}$). As shown in Fig. 4 and Table 4, n_c increases with the size of adsorbates A as expected. Notably two $n_{c,\beta}$ for CH_3NH in Table 4 are responsible for the two point contacts, and therefore the extent of electron overlapping is the mean of the two $n_{c,\beta}$. The repulsive AAIs E_{rep} for halogen have been obtained in a previous publication and is re-plotted verse n_c in Fig. 5. The optimal fitting functions of halogen adsorbates for α's and β's are $E_{rep,\ \alpha} = -39.9 + 44.2 \times \exp(n_{c,\alpha}/0.055)$, $E_{rep,\ \beta m} = -5.9 + 17.3 \times \exp(n_{c,\beta}/0.041)$, and $E_{rep,\ \beta p} = 11.0 + 6.0 \times \exp(n_{c,\beta}/0.022)$. The calculated interactions, regardless of adsorbate types, fall reasonably close to the fitted curves, indicating that the trend between E_{rep} and n_c is moderately consistent. Applying the n_c in Table 4 into these empirical equations, repulsive interactions $E_{rep,\ \alpha}$, $E_{rep,\ \beta m}$, $E_{rep,\ \beta p}$ can be obtained for each polar fragments A; they are also listed in Table 4. E_{rep} thus indicates that α interactions become significant for larger fragments such as CH_3O and CH_3NH.

3.4. Derivation and origin of the attractive adsorbate–adsorbate interactions

While the electron overlapping always leads to repulsive AAIs, some of the total interactions between two nearest neighboring polar adsorbates are attractive, as discussed in Section. 3.2. The crossover behavior shown in Fig. 3 suggests that a competing attractive interaction E_{att} exists between two neighboring polar adsorbates and the total interaction is the sum of the two interactions: $\alpha = E_{rep,\ \alpha} + E_{att,\ \alpha}$; $\beta = E_{rep,\ \beta} + E_{att,\ \beta}$. Given an α or β in Table 3, $E_{rep,\ \alpha}$ and $E_{rep,\ \beta}$ in Table 4, the attractive $E_{att,\ \alpha}$ and $E_{att,\ \beta}$ can be derived; they are listed in Table 5. The origins of these attractive interactions are yet to be elucidated.

As mentioned in Section 3.1, Fig. 1 shows that each adsorbate A_1 has one of its hydrogen atom (referred to as H_1) fairly close to an unshared pair of electrons of an oxygen or nitrogen atom (referred to as Y_2) in the nearest neighboring adsorbate A_2 in the same row. As Table 5 indicates, the distances between H_1 and Y_2, i.e. d_α, are around 3 Å for adsorbates OH, NH_2 and CH_3NH in the relevant Structures 3, 4, 7 and 8. The corresponding interaction strength, $E_{att,\ \alpha}$, is around −50 meV. Because the CH_3 group provides the enabling flexibility, adsorbates CH_3O have a markedly smaller d_α (2.3 Å) and, therefore, larger $E_{att,\ \alpha}$ of −78 meV. Fig. 1 and Table 5 also indicate that an H-bond is present for two neighboring NH_2 in two dimer rows. The distance $d_{\beta m}$ between H_3 and Y_1 is similar (~3 Å), so is the corresponding $E_{att,\ \beta m}$ (about −40 meV). These characteristics suggest that a weak H-bond is formed and that the H-bond is responsible for the attractive component in both α and β interactions.

Other distances ($d_{\beta m}$ and $d_{\beta p}$) listed in Table 5 for OH and CH_3O are typically larger than 3.5 Å and exceed the bond length of a typical H-bond. Although the corresponding $E_{att,\ \beta}$ are consequently smaller than $E_{att,\ \alpha}$, they are still substantial due to the strong dipole forces between the polar adsorbates.

Table 5
Adsorbate attraction energies E_{att} derived from α, β_p, β_m in Table 3 and $E_{rep,\ \alpha}$, $E_{rep,\ \beta m}$, $E_{rep,\ \beta p}$ in Table 4. Also listed are hydrogen bond length between an electronegative O (or N) atom and proton in two nearest neighboring adsorbates. d_α, $d_{\beta m}$ and $d_{\beta p}$ indicate the mean length and dispersion of H-bonds for relevant Structures (3, 4, 7, 8), (2, 4) and (6, 8), respectively.

A	E_{att} (meV)			Length of H-bonds (Å)		
	$E_{att,\ \alpha}$	$E_{att,\ \beta m}$	$E_{att,\ \beta p}$	d_α	$d_{\beta m}$	$d_{\beta p}$
OH	−52.0	−22.3	−37.0	3.05 ± 0.05	3.74 ± 0.45	3.64 ± 0.35
NH_2	−48.3	−35.7	−49.8	3.09 ± 0.10	3.07 ± 0.10	3.29 ± 0.05
CH_3O	−78.4	−13.1	−8.1	2.25 ± 0.10	4.30 ± 0.10	3.70 ± 0.25
CH_3NH	−43.5	−18.6		2.70 ± 0.15	2.96 ± 0.10	3.04 ± 0.10

4. Conclusions

The reactions of technologically relevant molecules such as water, ammonia, methanol, and methylamine with Si(100) involve dissociation into adsorbates H and A, where A are, respectively, OH, NH_2, CH_3O, and CH_3NH polar radicals. Between these polar adsorbates and other organic surface species, several interactions, both attractive and repulsive, can occur to each other. The separation of various contributions to the AAIs is a challenging task. Using DFT calculations, the present work examines the energetics of various ordered mixed adsorbate structures of several prototypical polar molecules on the Si(100) surface. The total nearest-neighbor and next-nearest-neighbor interactions between individual adsorbed polar fragments are extracted. The repulsive interactions are then separated from the total interactions by comparing the degrees of charge overlapping with that of halogen adsorbates. The differences between the total AAIs and the steric repulsions are found to be attractive. Examination of the atomic structures and charge distributions indicate that the attractive AAIs are due mainly to the hydrogen bonds or strong dipole–dipole interactions.

This finding suggests that the hydrogen bonding competes with direct adsorbate–adsorbate steric repulsion, which is significant for H_2O and NH_3 adsorption, and contributes to the alignment of dissociated OH and NH_2 species on the same side of dimers along a row. Due to the strong repulsive interactions between the adsorbates CH_3NH, the adsorbate–adsorbate repulsion (which is greater than the hydrogen-bonding energy) results in the zigzag arrangement of the CH_3NH species along a row at low temperatures (≦200 K), consistent with recent experimental observations. Between small (OH, NH_2) and large adsorbate (CH_3NH), the structure of dissociated CH_3O moieties exhibit an attractive-to-repulsive crossover behavior, that is, both the alignment of CH_3O on the same side and the zigzag arrangement along a row are energetically allowed.

Acknowledgment

The authors wish to acknowledge the financial support of National Science Council Taiwan under grant NSC 102-2112-M-007-008-MY3 (DSL). We are grateful to the National Center for High-Performance Computing of Taiwan for providing computational support.

Appendix A. Supplementary data

Supplementary data to this article can be found online at http://dx.doi.org/10.1016/j.susc.2014.12.002.

References

[1] Y. Wang, G.S. Hwang, J. Chem. Phys. 122 (2005) 164706.
[2] J.H.G. Owen, J. Phys. Condens. Matter 21 (2009) 443001.
[3] A. Bogicevic, S. Ovesson, P. Hyldgaard, B.I. Lundqvist, H. Brune, D.R. Jennison, Phys. Rev. Lett. 85 (2000) 1910.
[4] Y. Widjaja, C.B. Musgrave, J. Chem. Phys. 120 (2004) 1555.
[5] F. Tao, Pure Appl. Chem. 80 (2008) 45.
[6] C.L. Perrin, J.B. Nielson, Annu. Rev. Phys. Chem. 48 (1997) 511.
[7] P.A. Kollman, L.C. Allen, Chem. Rev. 72 (1972) 283.
[8] J.-H. Cho, K.S. Kim, S.-H. Lee, M.-H. Kang, Phys. Rev. B 61 (2000) 4503.
[9] A.B. Gurevich, B.B. Stefanov, M.K. Weldon, Y.J. Chabal, K. Raghavachari, Phys. Rev. B 58 (1998) R13434.
[10] J.J. Gallet, F. Bournel, F. Rochet, U. Köhler, S. Kubsky, M.G. Silly, F. Sirotti, D. Pierucci, J. Phys. Chem. C 115 (2011) 7686.
[11] C. Marilena, L. Karin, J. Phys. Condens. Matter 17 (2005) 1289.
[12] K.T. Queeney, Y.J. Chabal, K. Raghavachari, Phys. Rev. Lett. 86 (2001) 1046.
[13] M.Z. Hossain, Y. Yamashita, K. Mukai, J. Yoshinobu, Phys. Rev. B 68 (2003) 235322.
[14] Y. Wang, G.S. Hwang, Chem. Phys. Lett. 385 (2004) 144.
[15] Y.-H. Lin, H.-D. Li, H.-T. Jeng, D.-S. Lin, J. Phys. Chem. C 115 (2011) 13268.
[16] P.E. Blöchl, Phys. Rev. B 50 (1994) 17953.
[17] G. Kresse, D. Joubert, Phys. Rev. B 59 (1999) 1758.
[18] G. Kresse, Phys. Rev. B 62 (2000) 8295.
[19] G. Kresse, J. Hafner, Phys. Rev. B 49 (1994) 14251.
[20] J.P. Perdew, J.A. Chevary, S.H. Vosko, K.A. Jackson, M.R. Pederson, D.J. Singh, C. Fiolhais, Phys. Rev. B 46 (1992) 6671.
[21] H.J. Monkhorst, J.D. Pack, Phys. Rev. B 13 (1976) 5188.
[22] J.J. Boland, Adv. Phys. 42 (1993) 129.
[23] H.N. Waltenburg, J.T. Yates, Chem. Rev. 95 (1995) 1589.
[24] D.J. Chadi, Phys. Rev. Lett. 43 (1979) 43.
[25] K. Hata, Y. Shibata, H. Shigekawa, Phys. Rev. B 64 (2001) 235310.
[26] J.E. Northrup, Phys. Rev. B 47 (1993) 10032.
[27] N. Roberts, R.J. Needs, Surf. Sci. 236 (1990) 112.
[28] A. García, J.E. Northrup, Phys. Rev. B 48 (1993) 17350.
[29] C. Manzano, W.H. Soe, H. Kawai, M. Saeys, C. Joachim, Phys. Rev. B 83 (2011) 201302.
[30] K. Hata, S. Yoshida, H. Shigekawa, Phys. Rev. Lett. 89 (2002) 286104.
[31] C.-Y. Chang, H.-D. Li, S.-F. Tsay, S.-H. Chang, D.-S. Lin, J. Phys. Chem. C 116 (2012) 11526.
[32] J. Dabrowski, M. Scheffler, Appl. Surf. Sci. 56–58 (1992) 15.
[33] O. Warschkow, S.R. Schofield, N.A. Marks, M.W. Radny, P.V. Smith, D.R. McKenzie, Phys. Rev. B 77 (2008) 201305.
[34] M.P. Casaletto, R. Zanoni, M. Carbone, M.N. Piancastelli, L. Aballe, K. Weiss, K. Horn, Surf. Sci. 505 (2002) 251.
[35] A.J. Carman, L. Zhang, J.L. Liswood, S.M. Casey, J. Phys. Chem. B 107 (2003) 5491.
[36] W. Luo, K.A. Fichthorn, Phys. Rev. B 72 (2005) 115433.
[37] D.B. Laks, L.G. Ferreira, S. Froyen, A. Zunger, Phys. Rev. B 46 (1992) 12587.